DOI: https://doi.org/10.62985/j.huit_ojs.vol26.no2E.417

OPTICAL WIRELESS POWER TRANSFER BETWEEN OBLIQUE PLANES OF TRANSMITTERS AND RECEIVERS

Hoa Dinh Nguyen

Department of Automation Engineering, School of Electrical and Electronic Engineering, Hanoi University of Science and Technology, Vietnam

International Institute for Carbon-Neutral Energy Research (WPI-I2CNER), and Institute of Mathematics for Industry (IMI), Kyushu University, Fukuoka, Japan

Email: *hoa.nguyendinh2@hust.edu.vn*

Received: 15 January 2026; Revised: 5 March 2026; Accepted: 4 April 2026

ABSTRACT

This paper studies an optical wireless power transfer (OWPT) system, in which the transmitter is a set of LEDs belonging to a plane and the receiver is a small solar panel assumed to move within another plane that is not parallel with the transmitter plane. Owing to the nonlinearity and non-convexity of the DC gain of the OWPT efficiency from each LED to the solar panel, the transmission efficiency of the overall OWPT system is also a nonlinear and non-convex function of the transmitting distances. It is therefore challenging to determine the optimal relative position between the LEDs and the solar panel such that the OWPT efficiency of the whole system is maximal. Some initial results on this problem will be presented in current research with simulations and demonstrated with realistic experiments.

Keywords: Optical wireless power transfer, LEDs, solar cells, nonlinear optimization, non-convex optimization.

1. INTRODUCTION

Internet-of-thing (IoT) and consumer electronic (CE) devices have been increasingly utilized in different industrial fields and our daily lives. A lot of examples of such devices can be found in wireless sensor networks, smart home appliances, wearables, smartphones, etc. With the rapid advancement of technologies nowadays, the size, cost, and energy consumption of IoT and CE devices have been significantly reduced, hence aid in the affordability for users. Therefore, the importance and popularity of those devices have recently become more obvious.

Since many IoT and CE devices will be deployed in the existing infrastructures, both outdoor and indoors, powering them is a notable issue. Wired power supply is a conventional method for doing so, but it suffers from several disadvantages. First, this method requires significant alteration to the existing infrastructures in order to make wired connections with power sources, hence incurring high costs and reducing the aestheticism. Second, many IoT and CE devices, e.g. wireless sensors, can be deployed at locations that are hard or inconvenient to access. Thus, other powering approaches are needed, for example harvesting ambient energy [1] or wireless power transfer (WPT) [2].

Harvesting ambient energy, e.g., solar [3], wind [4], temperature [5], and mechanical vibration [6], is a nice approach for powering IoT and CE devices. Nevertheless, it is only available under certain conditions, for instance, having enough sunlight, strong enough wind, or high enough differences in temperature or pressure. As such, this powering approach is not suitable in many places that do not possess those conditions, e.g., indoor environments in

homes, buildings, commercial facilities, etc.

WPT is another approach for supplying power to IoT and CE devices, under which the disadvantages of the wired and ambient energy harvesting methods are avoided. Especially, WPT can be employed for both indoor and outdoor environments, hence offering a great way for powering such devices. It is noteworthy that there are several different WPT technologies [7] such as inductive WPT (IWPT) [8], capacitive WPT (CWPT) [9], microwave WPT (MWPT) [10], and optical WPT (OWPT) [11-14]. While IWPT, resonant IWPT, and CWPT are limited to short transmitting ranges, typically within tens of centimeters, MWPT and OWPT are able to wirelessly transmit power to much further distances.

In the current research, the problem of powering small indoor IoT and CE devices is investigated. For this problem, all the WPT technologies mentioned above could be candidates. However, at small power scales and small system sizes, the energy efficiency of IWPT, CWPT, and MWPT technologies is lower than that of the OWPT technology [16-18]. Furthermore, the transmitting distance in the context of small system sizes, if using IWPT or CWPT, is very short, usually within several centimeters. Last but not least, additional system components, e.g. transmitters and related circuits, must be equipped, if IWPT, CWPT, or MWPT are utilized, leading to higher system size, cost, and complexity. Hence, OWPT would be the most suitable WPT technology in this context.

In OWPT systems, optical transmitters can be classified into two types, laser and light emitting diode (LED), with tradeoffs between them. Light output of the first type, laser, is highly focused and has high intensity, therefore can deliver more power and over a longer distance than that of the second type, LEDs. As such, there have been a number of studies on using laser-based OWPT for IoT devices, e.g., [15], [19-22]. The problem of optimal scheduling for simultaneously charging multiple IoT devices using a resonant laser beam technique was investigated in [15]. In [19], the effects of the laser beam deformation and the solar cell module configuration on the performance of an indoor OWPT system were analyzed. Resonant beam utilizing retroreflectors for OWPT was studied in [20] based on the transfer matrix. The idea of using unmanned aerial vehicles (UAVs) as mobile optical transmitters in OWPT systems has recently been researched in [21], [22]. Note, however, that OWPT systems using lasers typically have larger size, higher complexity and cost, because of many optical components for laser beam generation and its safety protection [23].

Meanwhile, OWPT systems utilizing LEDs have better tolerance to transmitter-receiver misalignment, owing to the wide light spreading angle of LEDs. Additionally, LEDs are usually safer than lasers, due to the low intensity of their outputs. Thus, OWPT systems employing LEDs have recently attracted many studies, e.g., [12-14], [24-26]. In [24] and [25], the designs of high-power LED arrays and related lenses were considered in order to achieve expected performance such as received output powers, transmitting distances, etc. Nevertheless, additional devices in LED-based OWPT systems such as optical lenses in [24], [25] also lead to higher system complexity and cost, larger sizes, and worse tolerance to transmitter-receiver misalignments.

This research therefore proposes to use the existing indoor LED lighting systems as optical transmitters in OWPT systems for indoor IoT and CE devices, without additional optical lenses, while small solar panels are utilized as optical receivers. The specific contributions of this research are as follows.

- A nonlinear and non-convex optimization problem is introduced, for the first time, when the planes of optical transmitters and receivers are oblique.
- Interesting results from simulations and experimental tests are presented. Simulation results depict significant differences with that of parallel planes of transmitters and receivers in existing research. On the other hand, realistic experiment results show that OWPT is feasible

between oblique planes of transmitters and receivers, even when the oblique angle is 90 degrees.

The remaining parts of this paper are as follows. The problem formulation is presented in Section 2. An initial theoretical investigation and illustrative simulation results are provided in Section 3. Then, realistic experiments with commercial LEDs and a small solar panel are given in Section 4. Lastly, conclusions and future work are given in Section 5.

2. PROBLEM DESCRIPTION

Denote η_t, η_r and η_e the energy efficiency of the transmitter, the receiver, and the transmitting environment, respectively. Then the overall efficiency of the considering OWPT system, denoted by η_{sys}, is calculated by:

$$\eta_{sys} = \eta_t \times \eta_r \times \eta_e \tag{1}$$

As such, given the transmitter output power P_t, the received power at the output of the receiver P_r is computed by:

$$P_r = \eta_{sys} \times P_t \tag{2}$$

It is worth emphasizing that η_e depends on the light source, i.e. the optical transmitter, and the transmitting environments. When the transmitter is an LED and the transmitting environment is the air, η_e can be estimated by the line-of-sight (LOS) DC gain of the optical link [12-14], as follows.

$$\eta_e = \begin{cases} \frac{(m_l+1)A}{2\pi d^2} \cos^{m_l} \phi \; g_f(\varphi) g_c(\varphi) \cos\varphi : 0 \le \varphi \le \varphi_w \\ 0 : \varphi > \varphi_w \end{cases} \tag{3}$$

The variables in (3), depicted in Fig. 1, are as follows. The transmission distance is denoted by d, while A represents the physical area of the optical receiver. The angle of incidence (i.e. the angle at which the receiver sees the transmitter) and the angle of irradiance (i.e. the angle at which the transmitter sees the receiver) are denoted by φ and ϕ, respectively. $g_f(\varphi)$ and $g_c(\varphi)$ are the gain of an optical filter and an optical concentrator, if exist, whereas φ_w is the optical receiver's width of the field of view (FOV). Lastly, m_l indicates the order of Lambertian emission given by the semi-angle at half illuminance $\Phi_{1/2}$ of an LED:

$$m_l = -\frac{\ln 2}{\ln(\cos \Phi_{1/2})} \tag{4}$$

The non-LOS gains of optical paths, e.g. reflections by walls, surrounding objects, etc., are not taken into account, because they are much smaller than the LOS gain while their modeling is much more complicated.

When the transmitter consists of an LED array, then (2) is valid for the optical link DC gain of each LED in the array. Subsequently, if the optical receiver is within the illumination ranges of several LEDs, then the optical receiver output power will be the sum of the output powers obtained by individual LEDs. This linear property of solar cell optical receivers was shown, e.g. for perovskite solar cells in our previous research [12]. Suppose that there are n LED transmitters whose belonging plane is in parallel with the surface of the solar cell, and whose illumination ranges cover the solar cell. Then the DC gain of the optical link established by an LED array is given by:

$$\frac{A}{2\pi} \sum_{i=1}^{n} \frac{(m_{l,i}+1)}{d_i^2} \cos^{m_{l,i}} \phi_i \cos\varphi_i \tag{5}$$

where i is the LED transmitter index, d_i is the distance from the i-th LED to the solar cell, as illustrated in Fig. 2(a), and the gains of optical filters and concentrators are omitted for

simplicity. For LEDs in an LED lighting array, their semi-angles at half illuminance are usually the same, hence (5) is simplified to be the following:

$$\frac{(m_l+1)A}{2\pi}\sum_{i=1}^{n}\frac{1}{d_i^2}\cos^{m_l}\phi_i\cos\varphi_i \qquad (6)$$

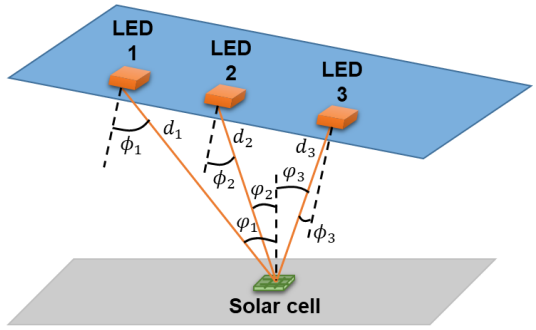

Fig. 1. Illustration for an OWPT system with the transmitter being a set of LEDs and the receiver being a solar cell, and the planes of the transmitter and receiver are oblique.

3. MAXIMAL EFFICIENCY PROBLEM SOLUTION AND ILLUSTRATIVE SIMULATION

As mentioned before, one of the goals in the considering OWPT system is to find out locations of the solar cell receiver to receive maximal wireless optical power from LEDs. In other words, the OWPT system efficiency in (6) should be maximized, and the features of the optimal solutions of (6) need to be analyzed, which will be presented in the following sections.

3.1. Theoretical Approach to Find Optimal Receiver Position

Assume that the plane of LED transmitters including the positions of LEDs is fixed, whilst the solar cell receiver plane is varied. Consequently, the maximal efficiency problem of the considering OWPT system between oblique planes of optical transmitters and receivers is described by the following non-convex geometric optimization programming, after explicitly computing the cosine terms in (6):

$$\begin{aligned} &\max && \sum_{i=1}^{n}\frac{z^m}{d_i^{m+3}} && (7)\\ &\text{s.t.} && ax+by+cz=h \end{aligned}$$

This optimization problem is more general than and different from that in [27] in two aspects. First, the cost function is more complicated than that in [27]. Second, it is a constrained optimization problem, whereas that in [27] was an unconstrained programming. As a result, resolving (7) is more difficult than finding the solution of the unconstrained optimization problem in [27].

Denote λ the Lagrange multiplier associated with the constraint in (7), then a Lagrangian function can be defined for (7) by:

$$L(x,y,z,\lambda)=-\sum_{i=1}^{n}\frac{z^m}{d_i^{m+3}}+\lambda(ax+by+cz-h)$$

The first-order necessary optimality conditions dictates that at the optimal point the following conditions are satisfied:

$$\frac{\partial L}{\partial x}=0,\frac{\partial L}{\partial y}=0,\frac{\partial L}{\partial z}=0$$

which result in a set of nonlinear equations to be solved together with the equality constraint in (7). Numerical methods then can be employed to obtain solutions of such a set of equations, i.e., the optima and the Lagrange multiplier of (7). Due to space limitation, details of those numerical methods are omitted here.

3.2. Illustrative Simulations

In this section, simulations are carried out to illustrate the presented OWPT above. More specifically, an office model is employed in which LEDs are hung on the room ceiling, while a plane with dimensions 2.5 m x 2.5 m is considered as the receiver plane. The ceiling LED array, which is at the center of the room, contains 4 rows, each row consists of 112 LEDs. The distance between two LEDs in a row is 1 cm, between two rows in a pair is 1 cm, and between two row pairs is 10 cm. Suppose that each LED has an output power of 100 mW, a semi-angle at half illuminance of 70 degrees. On the other hand, the optical receiver has a physical area of 2.5 cm^2 and an FOV of 60 degrees.

Consider the context in which the receiver plane has a normal vector $[0.1, 0.2, 1]^T$. First, assume that a point (0.1, 0.3, 0.07) lies in the receiver plane, then its equation is described by: $0.1x + 0.2y + z = 0.13$. The receiver plane is depicted in Fig. 2(a). Subsequently, the optical power distribution on the receiver plane is shown in Fig. 2(b). It can be clearly seen that the wireless optical power distribution is asymmetric, due to the obliqueness of the receiver plane to the transmitter plane, unlike that in [27] where the planes of transmitters and receivers are parallel.

Then consider when a point (0.1, 0.3, 0.3) belongs to the receiver plane. The plane equation in this scenario is: $0.1x + 0.2y + z = 0.37$. The corresponding simulation results are shown in Fig. 3(a) and Fig. 3(b). It can be seen that when the z-value of the initial point is increased, while the other values on x and y axis remain unchanged, the number of local maxima decreases from three to one, although the wireless optical power distribution in both cases is asymmetric.

Lastly, let us investigate the optical wireless power distribution when the relative distance between the transmitter and receiver planes is large. In particular, assume that a point (0.1, 0.3, 0.7) is on the receiver plane, making the receiver plane equation be: $0.1x + 0.2y + z = 0.77$. Simulation results in this case are displayed in Fig. 4(a) and Fig. 4(b) for the receiver plane and the optical power distribution on it, respectively. Interestingly, the optical power distribution on the receiver plane becomes more symmetric, as clearly observe in Fig. 4(b). This pseudo-symmetry shape of optical power distribution is kept as the relative distance between the transmitter and receiver planes is bigger.

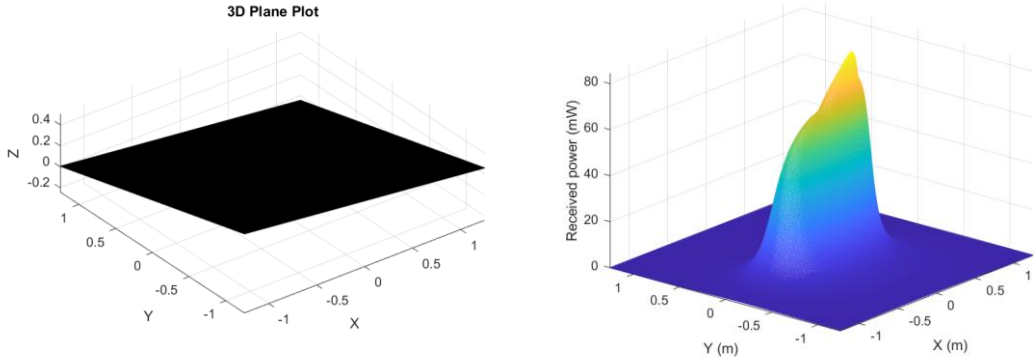

(a) (b)

Fig. 2. Simulation results for the illustrative example, simulation 1: (a) receiver plane; and (b) wireless optical power distribution on the oblique receiver plane.

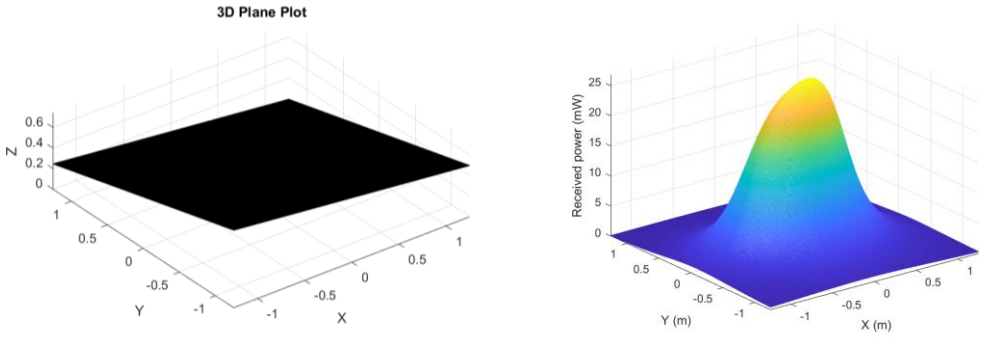

(a) (b)

Fig. 3. Simulation results for the illustrative example, simulation 2: (a) receiver plane; and (b) wireless optical power distribution on the oblique receiver plane.

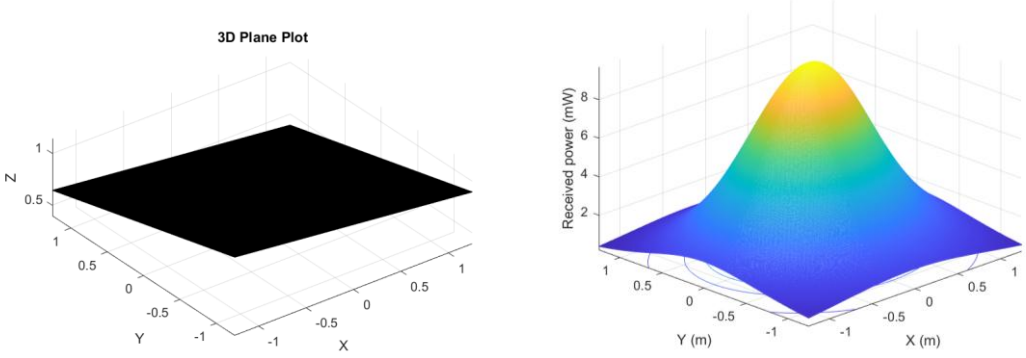

(a) (b)

Fig. 4. Simulation results for the illustrative example, simulation 3: (a) receiver plane; and (b) wireless optical power distribution on the oblique receiver plane.

4. EXPERIMENTAL TESTS

In this section, the capability of OWPT when the planes of transmitters and receivers are not parallel, but oblique is demonstrated. Experiments are performed using a small solar cell with dimensions 25mm x 25mm as the receiver and a commercial white-light desk lamp composing of 25 LEDs located in a line with a length of 26 cm as the transmitter, as depicted in Fig. 5. To visually confirm the OWPT, the output of the solar cell is connected to a small LED via a voltage boost circuit. Accordingly, the OWPT is successfully made if the above indicating LED is on, otherwise the OWPT was not made.

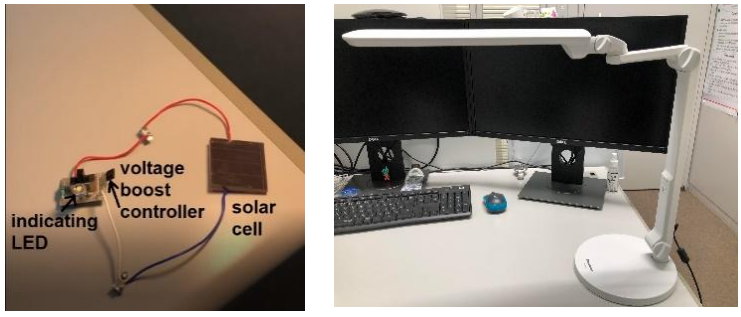

(a) (b)

Fig. 5. OWPT system used in the tests: (a) optical receiver; and (b) optical transmitter.

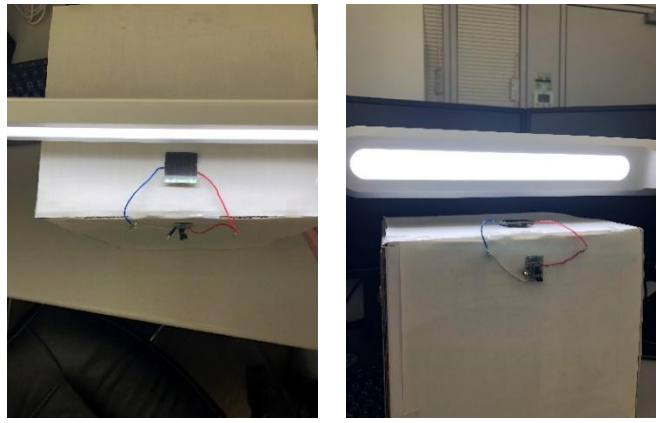

(a) (b)

Fig. 6. OWPT under a 75-degree obliqueness between the transmitter and receiver planes: (a) top view; (b) side view.

Note that the sizes of the LED transmitter and solar panel receiver will affect the OWPT performances. However, a detailed study on the effects of the transmitters and receivers is not considered in the current work, due to space limitation.

The ambient light conditions are not controlled nor considered, because the windows in the experiment room were fully covered with curtains. Hence, the results presented in the following were not affected by ambient lights. Moreover, the oblique angle between the transmitter and the receiver planes is limited to 90 degrees to reflect practical scenarios in reality. This angle is measured using a standard, commercial protractor.

First, the optical transmitter is rotated 75 degrees along the *x*-axis, but the relative distance between LEDs and the solar cell is not long, as exhibited in Fig. 6. In particular, the distance from the center of LED array to the solar cell is 4.5 cm. However, this is quite an extreme case, since the planes of the transmitter and receivers are nearly orthogonal. Despite such a challenging condition, the OWPT is still feasible that the indicating LED is lit. Similar success of OWPT is observed when the rotation angle along the *x*-axis varies from 0 to 75 degrees.

(a) (b) (c)

Fig. 7. OWPT under a 75-degree rotation along the *y*-axis: (a) the transmitter and receiver are aligned; (b) top view of unaligned transmitter and receiver; and (c) side view of unaligned transmitter and receiver.

Next, the LED-array transmitter is rotated along the *y*-axis and the relative distances between LEDs and the solar cell is made to be long, as illustrated by a 45-degree rotation along the *y*-axis in Fig. 7. It is then verified that the OWPT is also feasible in this tough scenario, even when the transmitter and receiver are misaligned by a distance of 20 cm, as shown in Fig. 7(b) and Fig. 7(c). Furthermore, the OWPT is available when the rotation angle along the *y*-axis is changed from 0 to 60 degrees. This, together with the results of the previous tests, indicates that OWPT is indeed feasible and realizable in reality for small devices, even when using low-power LED transmitters and indoor conditions. Therefore, this OWPT technology could be employed for many realistic applications such as for wirelessly powering internet-of-thing (IoT) and consumer electronic devices (e.g., smartwatches, smart rings, smart labels in supermarkets, etc.).

Finally, to further validate the above-mentioned point while being consistent with the simulations in Section III, experiments are conducted with a ceiling lighting system (in the same office as above tests) as the optical transmitter and the same solar cell as in Fig. 5(a) as the optical receiver. The configuration of such ceiling light is exactly the same as that described in the simulations in Section III. To begin, the solar cell receiver is put under and in parallel with the ceiling LED array, as displayed in Fig. 8. The distance between the transmitter and receiver planes is 160 cm, very far for OWPT with LEDs. Interestingly, the indicating LED is still ON, i.e., the OWPT is still available at such a long distance. This again demonstrates the viability and practicality of optical wireless charging for small devices, e.g., IoT and consumer electronic devices, by existing indoor lighting systems. Consequently, the solar cell optical receiver is mounted on an office wall, which is orthogonal to the ceiling LEDs, as shown in Fig. 9(a). The relative distance between the optical transmitter and receiver in this case is 52 cm along the *z*-axis and is 55 cm along the *x*-axis. Compared to the situation shown in Fig. 7, the OWPT system setup here is even more challenging, yet natural. A closer look at the optical receiver exhibited in Fig. 9(b) reveals that the OWPT is successful, where the indicating LED is ON.

Fig. 8. OWPT at a 160 cm distance between the ceiling LED array and the optical receiver.

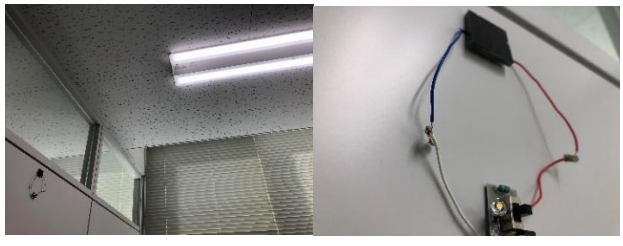

(a) (b)

Fig. 9. OWPT with wall-mounted optical receiver, 90-degree rotated to the ceiling LED-array transmitter: (a) the whole system view; (b) a closer view at the receiver with the lit indicating LED.

5. CONCLUSION

The current research has presented a study on an OWPT system consisting of a set of LEDs as the optical transmitter and a solar panel as the optical receiver. Moreover, the transmitter and receiver planes are not parallel. This results in a nonlinear, non-convex optimization problem for finding the optimal relative location of the receiver to the transmitter at which the overall wireless energy transmitting efficiency is maximal. This optimization problem is even more difficult than that introduced in a recent work in the literature. As such, resolving it and analyzing its properties are interesting but challenging. An initial theoretical analysis is then provided in this work, illustrated by simulations and demonstrated by realistic experiments. While simulation results indicate significant differences with the previous research in which the transmitter and receiver planes are parallel, experimental tests show that OWPT between oblique planes of transmitters and receivers, as investigated in this research, is indeed feasible. Hence, this technology could be employed for self-powering of small indoor devices such as IoT and consumer electronic devices.

Our ongoing study is investigating the analytical solutions of the set of nonlinear equations resulted from the first-order optimality condition for the above-mentioned nonlinear, non-convex programming. Features of the optimal points are also being researched using bifurcation theory. Results obtained from these works will be reported in the future.

Acknowledgment: This research is funded by Hanoi University of Science and Technology (HUST) under project number T2025-XS-001. The author would also like to sincerely thank International Institute for Carbon-Neutral Energy Research (WPI-I2CNER) and Institute of Mathematics for Industry (IMI), Kyushu University, Fukuoka, Japan, for inviting the author as a Visiting Professor and for providing facilities at which the OWPT experimental tests in Section 4 were carried out.

REFERENCES

[1] H. Jayakumar, K. Lee, W. S. Lee, *et al.*, "Powering the Internet of Things," in *Proc. 2014 Int. Symp. Low Power Electron. Des. (ISLPED)*, New York, NY, USA, 2014, pp. 375–380, doi: https://doi.org/10.1145/2627369.263164

[2] T. Helgesen and M. Haddara, "Wireless Power Transfer Solutions for 'Things' in the Internet of Things," in *Future Technologies Conference (FTC 2018)*, K. Arai, R. Bhatia, and S. Kapoor, Eds., vol. 880, *Advances in Intelligent Systems and Computing*. Cham, Switzerland: Springer, 2019, pp. 92–103, doi: https://doi.org/10.1007/978-3-030-02686-8_8

[3] R. Haight, W. Haensch, and D. Friedman, "Solar-Powering the Internet of Things," *Science*, vol. 353, no. 6295, pp. 124–125, 2016, doi: https://doi.org/10.1126/science.aag047

[4] H. Sun *et al.*, "MEMS-Based Energy Harvesting for the Internet of Things: A Survey," *Microsyst. Technol.*, vol. 24, no. 7, pp. 2853–2869, 2018, doi: https://doi.org/10.1007/s00542-018-3763-z

[5] G. Hu, H. Edwards, and M. Lee, "Silicon Integrated Circuit Thermoelectric Generators With a High Specific Power Generation Capacity," *Nat. Electron.*, vol. 2, no. 7, pp. 300–306, 2019, doi: https://doi.org/10.1038/s41928-019-0271-9

[6] K. Paul, A. Amann, and S. Roy, "Tapered Nonlinear Vibration Energy Harvester for Powering Internet of Things," *Appl. Energy*, vol. 283, Art. no. 116267, 2021, doi: https://doi.org/10.1016/j.apenergy.2020.116267

[7] D. H. Nguyen and A. Chapman, "The potential contributions of universal and ubiquitous wireless power transfer systems towards sustainability," *Int. J. Sustain. Eng.*,

vol. 14, no. 6, pp. 1780–1790, Oct. 2021, doi: https://doi.org/10.1080/19397038.2021.1988187

[8] S. Kisseleff, I. F. Akyildiz and W. H. Gerstacker, "Survey on Advances in Magnetic Induction-Based Wireless Underground Sensor Networks," *IEEE Internet Things J.*, vol. 5, no. 6, pp. 4843–4856, Dec. 2018, doi: 10.1109/JIOT.2018.2870289.

[9] A. M. Jawad *et al.,* "Opportunities and Challenges for Near-Field Wireless Power Transfer: A Review," *Energies*, vol. 10, no. 7, 2017, Art. no. 1022, doi: https://doi.org/10.3390/en10071022

[10] W. Lin, R. W. Ziolkowski and J. Huang, "Electrically Small, Low-Profile, Highly Efficient, Huygens Dipole Rectennas for Wirelessly Powering Internet-of-Things Devices," *IEEE Trans. Antennas Propag.*, vol. 67, no. 6, pp. 3670–3679, Jun. 2019, doi: https://doi.org/ 10.1109/TAP.2019.2902713

[11] X. Liu, N. Ansari, Q. Sha and Y. Jia, "Efficient Green Energy Far-Field Wireless Charging for Internet of Things," *IEEE Internet Things J.*, vol. 9, no. 22, pp. 23047-23057, Nov. 2022, doi: https://doi.org/10.1109/JIOT.2022.3185127

[12] D. H. Nguyen, G. Tumen-Ulzii, T. Matsushima and C. Adachi, "Performance Analysis of a Perovskite-Based Thing-to-Thing Optical Wireless Power Transfer System," *IEEE Photonics J.*, vol. 14, no. 1, Art no. 6213208, Feb. 2022, doi: https://doi.org/ 10.1109/JPHOT.2022.3146365

[13] D. H. Nguyen, T. Matsushima, C. Qin and C. Adachi, "Toward Thing-to-Thing Optical Wireless Power Transfer: Metal Halide Perovskite Transceiver as an Enabler," *Front. Energy Res.*, vol. 9, Art. no. 679125, Jun. 2021, doi: https://doi.org/10.3389/fenrg.2021.679125

[14] D. H. Nguyen, "Optical Wireless Power Transfer for Moving Objects as A Life-Support Technology," in *Proc. of 2020 IEEE 2nd Global Conference on Life Sciences and Technologies (LifeTech)*, Kyoto, Japan, 2020, pp. 405–408, doi: https://doi.org/10.1109/LifeTech48969.2020.1570618863

[15] W. Fang, Q. Zhang, Q. Liu, J. Wu and P. Xia, "Fair Scheduling in Resonant Beam Charging for IoT Devices," *IEEE Internet Things J.*, vol. 6, no. 1, pp. 641–653, Feb. 2019, doi: https://doi.org/10.1109/JIOT.2018.2853546

[16] G-H Lee *et al.,* "Multifunctional materials for implantable and wearable photonic healthcare devices," *Nat. Rev. Mater.*, vol. 5, pp. 149–165, 2020. doi: https://doi.org/10.1038/s41578-019-0167-3

[17] L. M. Wangatia, S. Yang, F. Zabihi, M. Zhu, S. Ramakrishna, "Biomedical electronics powered by solar cells," *Curr. Opin. Biomed. Eng.*, vol. 13, pp. 25–31, 2020, doi: https://doi.org/10.1016/j.cobme.2019.08.004

[18] N. Wuthibenjaphonchai, M. Haruta, K. Sasagawa, T. Tokuda, S. Carrara, J. Ohta, "Wearable and Battery-Free Health-Monitoring Devices With Optical Power Transfer," *IEEE Sens. J.*, vol. 21, no. 7, pp. 9402–9412, 2021. doi: https://doi.org/ 10.1109/JSEN.2021.3050139

[19] J. Tang, K. Matsunaga, and T. Miyamoto, "Numerical analysis of power generation characteristics in beam irradiation control of indoor OWPT system," *Opt. Rev.*, vol. 27, no. 2, pp. 170–176, 2020. doi: https://doi.org/10.1007/s10043-020-00590-z

[20] Y. Bai, Q. Liu, R. Chen, Q. Zhang and W. Wang, "Long-Range Optical Wireless Information and Power Transfer," *IEEE Internet of Things Journal*, vol. 10, no. 2, pp. 1617–1627, Jan 2023, doi: https://doi.org/10.1109/JIOT.2022.3209588

[21] M. R. Hassan, "Theory of Dronized Laser Source for Next Generation of Optical Wireless Power Transmission," *IEEE J. Sel. Top. Quantum Electron.*, vol. 28, no. 5, Art. no. 6700109, Sep.–Oct. 2022, doi: https://doi.org/10.1109/JSTQE.2022.3162170

[22] J. Chen and X. Liu, "Profit-Driven UAV Green Wireless Charging for WSN," in *Proc. 2022 IEEE Int. Conf. Smart Internet Things (SmartIoT)*, Suzhou, China, 2022, pp. 1–6, doi: https://doi.ieeecomputersociety.org/10.1109/SmartIoT55134.2022.00010.

[23] W. Fang *et al.,* "Safety Analysis of Long-Range and High-Power Wireless Power Transfer Using Resonant Beam," *IEEE Trans. Signal Process.*, vol. 69, pp. 2833–2843, 2021, doi: https://doi.org/10.1109/TSP.2021.3076893

[24] M. Zhao, T. Miyamoto, "1 W High Performance LED-Array Based Optical Wireless Power Transmission System for IoT Terminals," *Photonics*, vol. 9, no. 8, 2022, Art. no. 576. doi: https://doi.org/10.3390/photonics9080576

[25] M. Zhao and T. Miyamoto, "Optimization for Compact and High Output LED-Based Optical Wireless Power Transmission System," *Photonics*, vol. 9, no. 1, Art. no. 14, 2022, doi: https://doi.org/10.3390/photonics9010014

[26] D. H. Nguyen, "Optical Wireless Power Transfer for Implanted and Wearable Devices," *Sustainability*, vol. 15, no. 10, Art. no. 8146, 2023, doi: https://doi.org/10.3390/su15108146

[27] D. H. Nguyen and K. Matsue, "Analysis of Optima Set in a Class of Non-Convex Geometric Optimization Problems Using Bifurcation Theory," *J. Optim. Theory Appl.*, vol. 207, no. 1, Art. no. 68, 2025, doi: https://doi.org/10.1007/s10957-025-02829-8.